International Journal of Current Pharmaceutical Research

ISSN- 0975-7066 Vol 8, Issue 3, 2016

Original Article

HOMOLOGY MODELING AND DEVELOPMENT OF DIHYDRODIPICONILATE REDUCTASE INHIBITORS OF *KLEBSIELLA PNEUMONIA*: A COMPUTATIONAL APPROACH

BAKI VIJAYA BHASKAR[1], TIRUMALASETTY MUNI CHANDRA BABU[1], WUDAYAGIRI RAJENDRA*[1]

[1]Division of Molecular Biology, Department of Zoology, Sri Venkateswara University, Tirupati 517502
Email: rajendraw2k@yahoo.co.in

Received: 20 Mar 2016, Revised and Accepted: 20 Jun 2016

ABSTRACT

Objective: In order to development of novel, potent and selective inhibitors of Dihydropiconilate reductase (KpDHDPR) of multidrug resistant *Klebsiella pneumonia.*

Methods: Protein sequence of KpDHDPR was retrieved from the UNIPROT and the primary and secondary structure was analyzed using Prot Param, SOPMA, GOR4 and Chou and Fasman. Afterword's, 3D structure of KpDHDPR was built by using MODELLEER$_{9.14.}$ The Molecular dynamics simulation was carried out using NAMD$_{2.9}$ with CHARMM27 force field for 10 picoseconds and production run with for 400 picoseconds time period covered with water box. Molecular docking and virtual screening was carried out using Auto Dock Vina$_{4.0}$ with PyRx interface. Bond angles, bond lengths, bond distances and binding interactions were analyzed using PyMol. Toxicity assessment and Lipinski rule of five of ligand were assessed using MOLINSPIRATION and OSIRIS Server.

Results: 3D structure of KpDHDPR was resolved on the basis of EcDHDPR that revealed N-terminal nucleotide domain and C-terminal substrate binding domain which are connected by a short hinge region. Nucleotide binding domain is formed with seven α-helices and the Substrate binding domain is composed with three α-helices and Rossman fold is observed with four α-helices and seven β-strands. Molecular docking analysis revealed that NADPH has exhibited more binding affinity to KpDHDPR than NADH. As results of virtual screening and docking, six compounds viz. ZINC04280533, ZINC04280532, ZINC04280468, ZINC33378709, ZINC05280538 and ZINC25694354 were identified. Bioavailability of these inhibitors are comply with the Lipinski rule of five, good pharmacokinetic and drug likeness properties.

Conclusion: In conclusion, *in silico* studies revealed that these lead scaffolds could helpful in the development of KpDHDP R inhibitors. Hence, these drug candidates might be promoted as promising antibacterial agents for the treatment of drug resistant gram negative bacterial infections.

Keywords: Dihydropiconilate reductase, NADH and NADPH, Homology Modeling, Docking, Virtual screening

© 2016 The Authors. Published by Innovare Academic Sciences Pvt Ltd. This is an open access article under the CC BY license (http://creativecommons.org/licenses/by/4.0/)

INTRODUCTION

Klebsiella pneumonia is multidrug resistant gram negative and nosocomial pathogen which possesses the greater threat of infections that are truly untreatable [1]. *K. pneumonia* is frequently resistant to several antibiotics viz. penicillins, cephalosporins, carbapenems, monobactams, quinolones, aminoglycosides tetracyclines and polymyxins. However, bacteria possess a variety of mechanism arise like deactivation of drugs, mutations in target enzyme, the petite permeability of the outer membrane, elevated expression of efflux pumps and R-plasmids with numerous resistance genes to deny the antimicrobials and antibiotics. Currently, several resistant genes, different virulence factors, drug candidates, essential metabolisms and pathogenesis of bacteria have been reported by genomics and proteomics approach. Several unique molecular targets have been identified from numerous pathways such as DNA replication, regulation, repair, protein synthesis, peptidoglycan synthesis, folic acid synthesis and amino acids synthesis, etc.

Diaminopimelate metabolism of bacteria provides various drug targets for the development of antibiotic design [2]. Among these, the biosynthesis of L-lysine is one of the crucial and unique metabolic pathway for transpeptidation of peptidoglycan and protein synthesis. L-lysine is synthesized from the precursor of L-aspartate by nine step pathway that L-aspartate is phosphorylated and reduced to L-aspartate-β-semi aldehyde with the assistance of dihydropiconilate synthase that is also intermediate for biosynthesis of methionine, threonine and isoleucine [3]. Further, 2, 3-dihydropiconilate (DHDP) is formed by aldol condensation of pyruvic and L-aspartate-β-semi aldehyde by dihydropiconialte synthase. The reduction of 2, 3-dihydropiconilate (DHDP) by dihydropiconilate reductase [4], gives rise to 2, 3, 4, 5 tetrahydropiconilate (THDP). Sequentially, tetrahydropiconilate is undergone transamination and epimerization via three divergent pathways leads to the yield of D, Ldiaminopamilate and lysine in both gram negative and positive bacteria [5].

So far, DHDPR crystal structures of *E. coli* (PDBID: 1DRU), *M. tuberculosis* (PDBID: 1YL5, 1C3V), *T. maritime* (PDBID: 1VM6), *B. thailandensis* (PDBID: 4F3Y), *Bartonellahenselae* (PDBID: 3IJP) *and S. aureus* (PDBID: 3QY9) in complexes with NADH/NADPH have been deposited in the Protein Data Bank. The structural design of DHDPR characterized as a homotetramer and each monomer composed of two domains such as N-terminal nucleotide binding domain (cofactor) which form Rossman fold and C-terminal substrate binding domain (tetramerization) which form open. Mixed α, β sandwich and two domains were linked through the flexible loop. However, DHDPR exhibits huge variations in the binding of nucleotide (NADH/NADPH) at the nucleotide binding pocket [6-8]. Active pocket is aligned in between these two domains and allow the catalysis by fetch the cofactor and substrate in close proximity. DHDPR doesn't have any mammalian counterparts and it is a very attractive potential target for the development of novel antibacterial agents and herbicides [9].

However, 2, 6pyridinedicarboxylic acid, Pyridine and piperidine derivatives and Dipicolinic acid were reported as DHDPR inhibitor with moderate activity and need to discover effective novel antibacterial agents especially with reference to drug resistance in bacteria [10, 11]. Keeping in view this, the present study explicates the structure of DHDPR of *K. pneumonia* strain HS11286 *(*KpDHDPR) and performed structure-based virtual screening in order to identify the novel scaffolds with structural variations and greater binding affinities.

MATERIALS AND METHODS

Primary and secondary structure analysis

The protein sequence of KpDHDPR strain HS11286 was retrieved from UNIPROT. Primary and Secondary structure elements were predicted PROTPARAM and different servers Viz. SOPMA [12], GOR4 [13] and Chou and Fasman [14].

Homology modeling

In order to explicate KpDHDPR structure, template structure was selected based on the highest sequence identity, high score, less e-value, highest resolution and R-factor by performing BLASTp against Protein Data Bank (PDB). Thus, the alignment of template and query sequence was performed by using ClustalX [15]. An ensemble of 3D KpDHDP Rmodels of were built using MODELLER [9, 14, 16].

Molecular dynamics (MD) simulation

The KpDHDPR model with the least DOPE score was selected for MD simulation using Nano-Molecular Dynamics ($NAMD_{2.9}$) software [17]. Force field of Chemistry of Harvard Molecular Modeling (CHARMM27) was used for lipids and proteins along with the TIP3P model for water [18]. Initially, protein was minimized with 250000 runs for 10 picoseconds followed by MD simulations were begun for 10, 00, 000 runs for 2ns. Integrated motion time step of 2fs was computed using multiple time step algorithms [19, 20]. Short range forces for every two-time step and long range forces for every four-time step were computed.

The pair list of the non-bonded interactions was computed with a pair list distance of 14.0 Å. Short-range interactions were defined as Vaander Waals and electrostatic interactions within 12 Å. Long-range electrostatic interactions were taken into an account using partial mesh ewald (PME) approach [21, 22]. The pressure was maintained at 1 atm using the Langevin piston and temperature at 300k was controlled using Langevin dynamics. Covalent interactions between hydrogen and heavy atoms were constrained using SHAKE/RATTLE algorithm [23, 24].

Model assessment

Ramachandran plot calculations using PROCHECK to check the stereochemical quality, environment profile using verify 3Dand non-bonded interactions using ERRAT were adopted [25, 26, 27]. The residue packing, atomic contacts and Z-score of Ramachandran plot were analyzed using WHAT IF and WHATCHECK [28]. Structure alignment of template and query models was performed by using SPDBV [29]. This final refined model was used for further docking analysis with selected compound.

Ligand preparation

Substrates (2, 3, 4, 5-tetradihydropiconilate and 2, 6 pyridines di-carboxylic acid (PDA)) and cofactors (NADH and NADPH) were downloaded from Pub Chem. PDA analogs were downloaded from ZINC database. All the ligands were added with hydrogen and energy minimized with Universal Force Field (UFF) using a Conjugate-gradient algorithm and used for docking studies.

Virtual screening and molecular docking

AUTODOCK $VINA_{4.0}$ couple with PyRx interface was used to carry out virtual screening and docking studies with ligands into the active pocket of DHDPR [30, 31]. Lamarkian Genetic Algorithm was used with the parameters: 150 Number of the individual population, the 25000Maximum number of energy evaluation, the 27000 Maximum number of top generation individuals to survive to next generation is 1, Gene mutation rate of 002, Crossover rate of 08, Cauchy beta of 10 and GA window size of 100.

The grid was set to at X=55.9962, Y=29.0573, Z=1.6822 and dimensions (Å) at X=55.9962, Y=29.0573, Z=1.6822 and exhaustiveness 8. The best-docked ligand conformations were tabulated and analyzed the binding interaction using PyMol [32].

Bioavailability

Lipinski rule of five such as cLogP, Molecular Weight, H-bond acceptor and H-bond donors and Toxicity risk assessment and overall Drug-score of compounds were predicted by using OSIRIS property explorer (http://www.organic-chemistry.org).

Table 1: Binding energy, bond distance and bond angles of lead molecules with the decisive residues of binding pocket of KpDHDP reductase

S. No.	Compounds	Protein-ligand interactions Protein Ligand	Distance	Bond angle	Binding energy
1	ZINC04280533	Phe79, Gly102, Phe106, Lys163, Phe243, Gly218, Glu219, Ala158, Thr170, Asn128, Glu219 Ala127 CA-N----------O32C	3.20	116.23	-11.3
2	ZINC04280532	Phe106, Lys111, Phe125, Ala126, Ala127, Asn134, Leu137, Lys138, Glu141, Gly169, Leu172, Ala173, Glu176, Ala177, Asp263, Met264, Arg265, Leu270.			-10.7
3	ZINC04280468	Thr103, Thr104, Gly105, Phe106, Lys111, Phe125, Ala126, Ala127, Leu137, Glu141, Gly169, Leu172, Ala173, Glu176, Ala177, Leu186, Ala186, Asp263, Arg265.			-10.7
4	ZINC33378709	Phe125 C-O----------O38C Gly105 CA-N----------O37C	3.49 3.31	139.18 81.07	-9.8
5	ZINC05280538	Lys111, Phe125, Ala126, Ala127, Asn134, Leu137, Lys138, Glu141, Gly169, Leu172, Ala173, Glu176, Ala177, Asp263, Arg265, Leu270.			-9.6
6	ZINC25694354	Phe79, Gly102, Thr104, Ala127, Asn128, Phe129, Lys163, Ser168, Gly169, Thr170, Arg212, val217, Phe243.			-9.0

Table 2: Bioavailability of KpDHDPR inhibitors were assessed by OSIRIS Server

S. No.	Compound	Mut	Tum	Irr	RE	ClogP	Solubility	MolWt	DL	DS
1	ZINC04280532	-	-	-	-	8.24	-10.26	408.0	-3.36	0.06
2	ZINC04280533	-	-	-	-	8.24	-10.26	408.0	-1.36	0.08
3	ZINC04280468	-	-	-	-	7.05	-8.66	358.0	-4.05	0.08
4	ZINC33378709	-	-	-	-	7.05	-8.66	358.0	-2.1	0.09
5	ZINC25694354	-	-	-	-	8.4	-10.24	490.0	-0.06	0.09
6	ZINC05280538	-	-	-	-	5.87	-7.05	308.0	-2.4	0.15

Mut: Mutagenic, Tum: Tumorigenic, Irr: Irritant, RE: Reproductive effect, DL: Drug-likeness, DS: Drug-score, logP: Partition coefficient, MW: Molecular weight, Sol: Solubility.

RESULTS AND DISCUSSION

Primary and secondary structures assessment

The protein sequence of KpDHDPR was taken from UNIPORT and analyzed physicochemical properties of Aliphatic index is 93.77, Grand average of hydropathicity is 0.050, Theoretical PI is 5.76, Extinction coefficient is 10095 and Instability index is 22.50 respectively. Secondary structure analysis has shown 41.76% alpha helix with 114 residues by SOPMA, 47.99% with 131 residues by GOR4 and 82.1% with 224 residues by Chou and Fasman respectively. The predicted values for extended strand were found to be 19.05% with 52 residues by SOPMA, 14.29% with 39 residues by GOR4 and 24.9% with 68 residues using Chou and Fasman respectively. Beta-turn exhibited 7.69% with 21 residues using SOPMA, 12.1% with 33 residues by Chou and Fasman while GOR4 was failed to identify beta turns. Random coil were found to be 31.50% with 86 residues by SOPMA, 37.73% with 103 residues by GOR4. Chou and Fasman fails to provide Random coils.

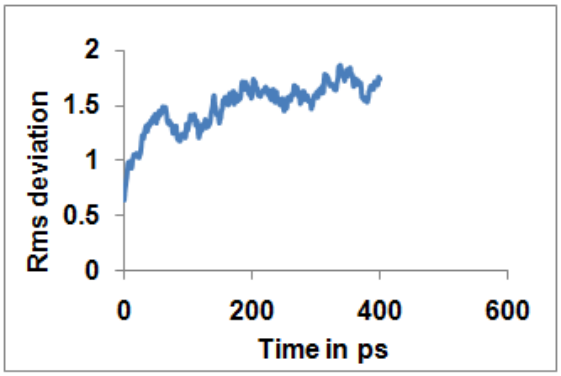

Fig. 1: Calculated RMSD graph of molecular dynamics simulations of KpDHDPR using NAMD2.9v. Graph was drawn between time was taken in X-axis and RMSD was taken in Y-axis

Homology modeling and MD simulation

In order to explicate the 3D KpDHDPR structure, comparative modeling was adopted using MODELLER[9.14]. Initially, template identification was carried out by performing similarity search by BLAST against PDB revealed that fourteen structure were hit from different bacterial species. Among these, EcDHPR (PDBID: 1ARZ) of *E. coli* has shown 92% of highest identity, 100% of Query coverage, e-value 2e-174, resolution 2.60Å and R-value 0.214 with the query sequence. Subsequently, Pairwise sequence alignment between template and query was achieved and Coordinates of structural conserved region, structurally variable region, N-terminal and C-terminal of template protein were assigned to query based on the satisfaction of spatial restraints. All the side chains were set by rotamer and a cluster of hundred KpDHDPR models was generated using MODELLER[9.14]. The lowest DOPE score value of model was subjected to MD simulation about 400 picoseconds. Trajectory graphs were plotted that showed root mean square deviation (RMSD) of the model revealed a sharp increase of 1.4 ps followed by minor fluctuations and achieved equilibrium around 2 ns (fig. 1). The final model was analyzed for binding pockets and structural comparison with EcDHDR was carried out and depicted in fig. 2a, b.

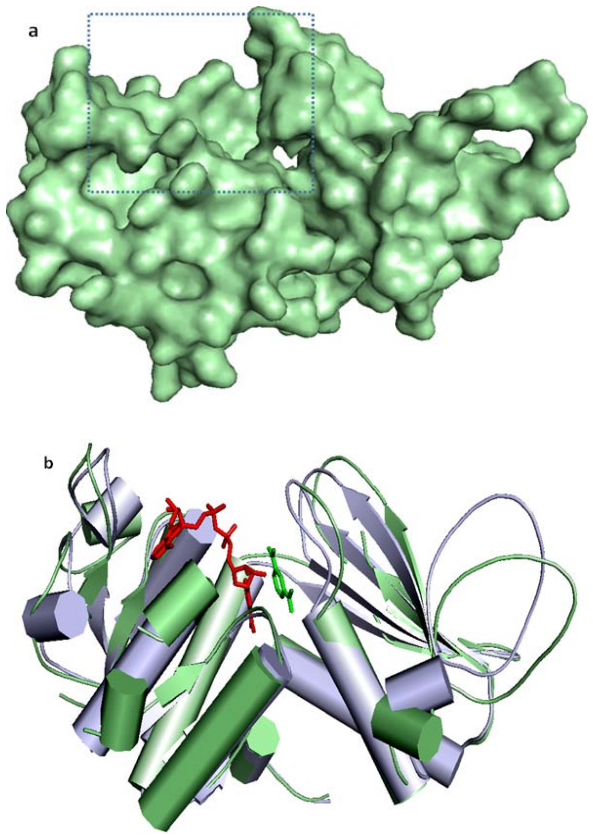

Fig. 2: (a). Surface model of KpDHDPR, (b). Superimposition of EcDHDPR and KpDHDPR and NADH (red) and 2, 6 PDC (green) are aligned its respective binding pockets

Model validation

The geometry of the final model was evaluated through Ramachandran plot calculations with PROCHECK that conferred 93.2% with 219 residues were aligned in most favored regions (A, B, L), 6.4% with 15 residues were allocated in additional allowed region, 0.4 % with 1 residues were found in generously allowed region and no residues in disallowed region respectively (fig. 3a).93.130% of the overall quality factor was observed with the use of ERRAT environment profile (fig. 3b). Verify-3D explicated that average 3D-1D score was over 0.2 revealed that the model was highly reliable (fig.3c). WHATCHECK program be evidence for the Z-score of 2nd generation packing quality is 1.922, Ramachandran plot manifestation is 0.104, chil/chi2 rotamer regularity 0.799 and bond length, bond angles, omega angle restraints, side chain planarity, improper dihedral distribution, Inside/Outside distribution are 0.946, 1.282, 0.777, 0.344, 0.812 and 0.984 were found to be good respectively.

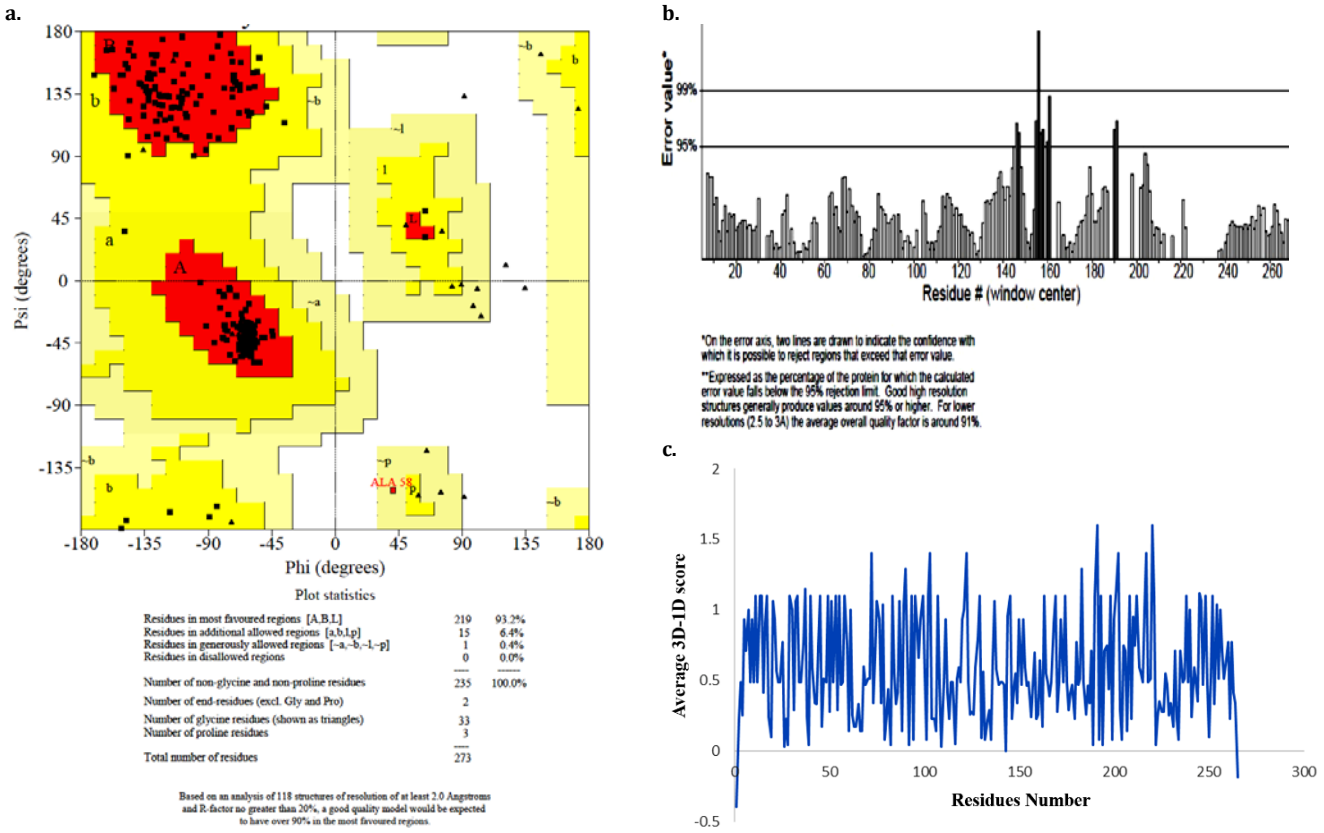

Fig. 3: (a) Ramachandran plot calculations of 3D-Model computed using PROCHECK, (b). 3D profiles of constructed 3D-model was verified using Erratprogramme. (c). Compatibility of atomic 3D-Model of its own amino acids residues (1D) using Verify3D server

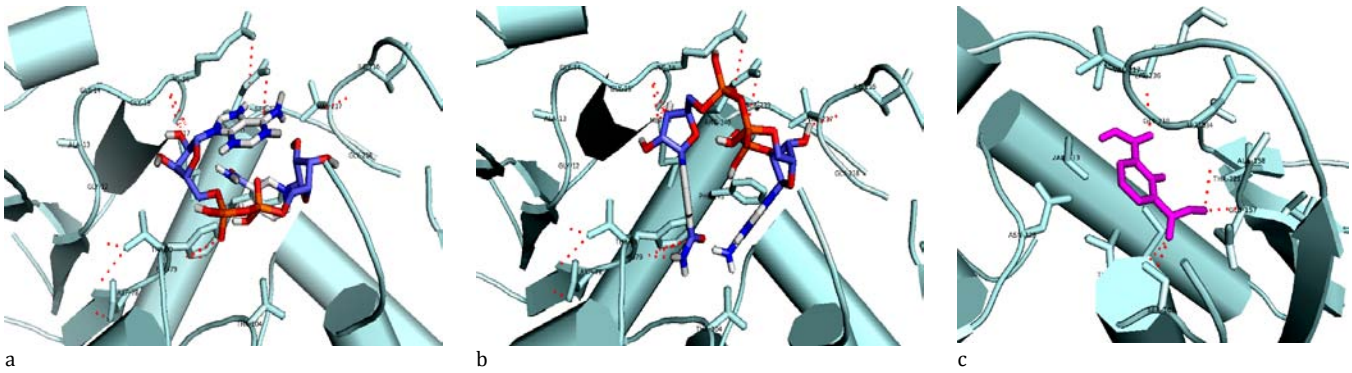

a b c

Fig. 4: Binding mode of a). NADH and b). NADPH were bound at the nucleotide binding domain whereas c). 2, 6 pyridine dicarboxylic acid was bound at the C-terminal domain of KpDHDPR

ZINC04280533 **ZINC04280532** **ZINC04280468**

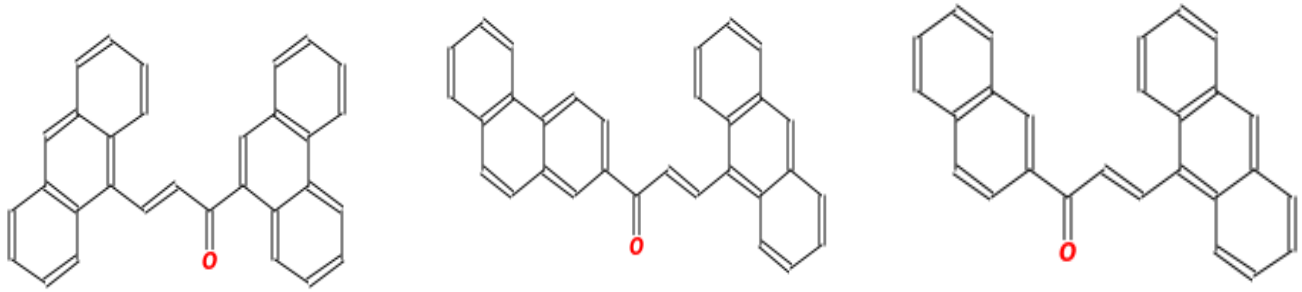

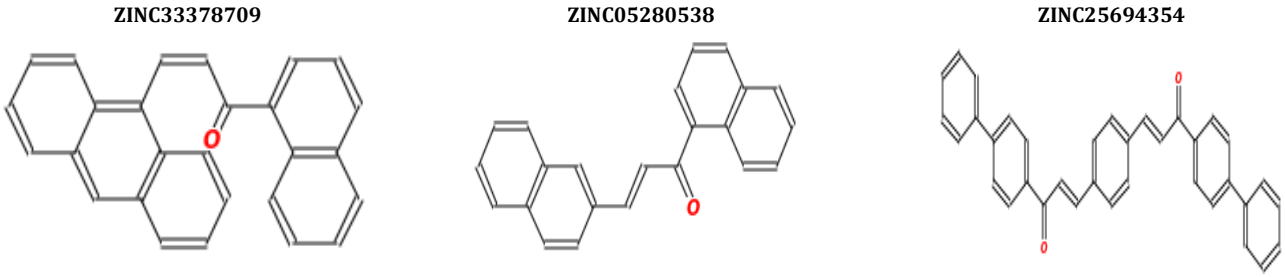

Fig. 5: 2D Structures of KpDHDPR inhibitors

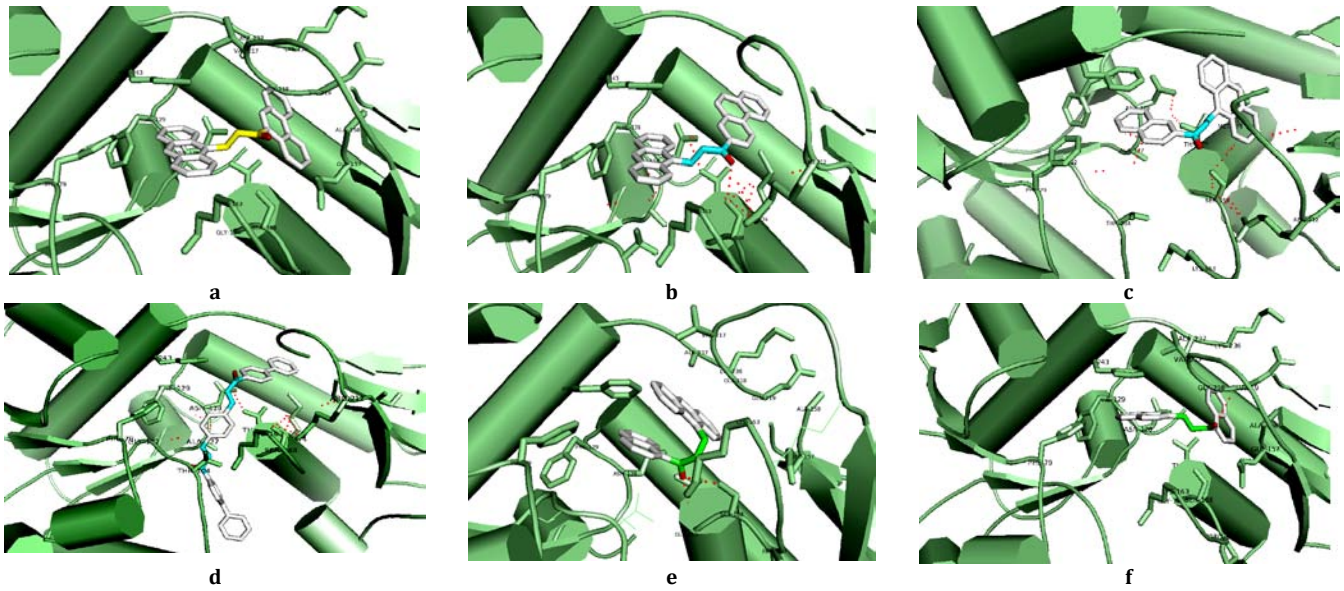

Fig. 6: Binding mode of a). ZINC04280533, b). ZINC04280532, c). ZINC04280468, d). ZINC33378709, e). ZINC25694354 and f). ZINC05280538 within the active pocket of KpDHDPR

KpDHDP Rmodel and substrate binding studies

KpDHDPR consists of 208 residues and possesses N-terminal nucleotide domain and C-terminal substrate binding domain which are connected by a short hinge region. N-terminal nucleotide binding domain is formed with seven α-helices Viz. αI (16-27), αII (43-52), αIII (66-70), αIV (82-95), αV (108-120), αVI (240-246) and αVII (262-268) and six β-sheets ranges from βI (6-10), βII (31-33), βIII (75-78), βIV (99-101), βV (122-125) and βVI (260-262) respectively. The C-terminal substrate binding domain is composed of three α-helices Viz. αI (131-150), αII (169-182), αIII (186-189) and four β-sheets Viz. βI (152-159), βII (207-212), βIII (219-226) and βIV (229-236) respectively. Rossman fold is observed with four helices and seven β-strands as monitored in the DHDPR's from various life forms. In order to accomplish the binding mode of 2, 3, 4, 5-tetradihydropiconilate, 2, 6-pyridine dicarboxylic acid (PDC), NADHand NADPH (fig. 4a, b, c). From the docking analysis, NADPH and NADH have shown binding affinity of-8.4 kcal/mol and-7.3 kcal/mol and interacted with key residues of Arg16, Arg39, Ser64, Asp78, Phe79, Thr80, Gly84, Thr85, Leu89 and Val217 at the nucleotide binding of N-terminal of KpDHDPR. 2, 6 pyridine dicarboxylic acid (PDC) has shown binding energy of-6.5 kcal/mol and interacted with Asn128, Glu157, Ser168, Gly169, Thr170, Arg212, Ile216, Thr221and Lys236 of the C-terminal domain of KpDHDPR.

Virtual screening and docking

Screening of ZINC compounds library using virtual screening and docking approaches to exploit complementary and eloquent interaction searches with binding pocket of KpDHDPR. VS screening study explicated six novel different scaffolds such as ZINC04280533, ZINC04280532, ZINC04280468, ZINC33378709, ZINC25694354 and ZINC05280538 possess highest binding affinity and displayed complementary interactions with active pocket residues of the C-terminal domain of KpDHDPR (table 1; fig. 5, 6). ZINC04280533 has shown highest binding affinity of-11.4 kcal/mol and exerted hydrophobic interactions through anthracene groups. ZINC04280532 and ZINC04280468 have exerted binding affinity of-10.7 kcal/mol and formed two interactions with Ser168 and displayed hydrophobic interactions between anthracene and naphthalene to Phe79, Phe129 and Phe243. ZINC33378709, ZINC05280538and ZINC25694354 have shown best binding affinities of-9.8, -9.6 and-9.6 kcal/mol. ZINC33378709 has biphenyl rings that interacted with PDC binding pocket whereas C=O group formed one interaction with Thr163. ZINC05280538 formed one interaction with Glu219 and had two naphthalene groups, one interacted with Phe129 and Phe243, another one interacted with Gly218 and Ala258. ZINC25694354 formed one interaction with Ser168 and had anthracene and naphthalene groups which interact through non-bonded interactions with active pocket.

Bioavailability

Drug-likeness properties will play an important role in the discovery of novel drugs and Pharmacodynamics, pharmacokinetics and toxicological aspects are important to resolves drug accessibility. Hitherto, lead molecules have shown eloquent pharmacodynamics properties with the active pocket of protein. Mainly drug-likeness depends upon the molecular features that compatible with absorption, distribution, metabolism and excretion in the body. Besides, Lipinski rule of five predictions as molecular weight (≤500), cLog (≤5), hydrogen bond acceptor (≤5) and hydrogen bond donor (≤5) of lead molecules revealed H-bond donors were predicted to be less than five and H-bond acceptors are less than ten. cLogP or

partition coefficient plays a major role in accessing the drug in the body which was found to be less than five and all the lead molecules were found to be satisfied that indicates compounds have the drug accessibility with good ADME properties. Moreover, extrapolation of toxicity properties through mutagenic, tumorigenic, irritant and reproductive effect conveyed all leads have not been found any adverse effect (table 2). Drug score is calculated for the above four risk factors which reveal that all the compounds displayed best drug score and could be helpful in the development of inhibitors for KpDHDPR.

CONCLUSION

In conclusions, comparative modeling, docking and virtual screening studies have been employed to explicate the potent novel KpDHDPRinhibitors for effective therapeutic applications in drug resistant gram negative bacterial infections. As a result of virtual screening and docking strategies, finally, six novels, potent and selective KpDHDPR inhibitors were identified. In addition, these lead candidates comply with the rule of five, no adverse effect and possess drug-likeness properties. Hence, these lead candidates might be promoted as promising antibacterial drugs for the generation of a rational discovery of novel, potent and selective inhibitors for KpDHDPR for the clinical management of multidrug-resistant bacteria.

ACKNOWLEDGEMENT

BVB is gratifying to University Grant Commission, New Delhi, India for providing financial support in the form of RGNF. All the authors are grateful to the Coordinator, Bioinformatics Infrastructure Facility, Department of Zoology, Sri Venkateswara University, Tirupati for providing bioinformatics facilities.

CONFLICT OF INTERESTS

All the authors declared that there is no conflict of interest

REFERENCES

1. Weigel LM, Steward CD, Tenover FC. gyrA mutations associated with fluoroquinolone resistance in eight species of enterobacteriaceae. Antimicrob Agents Chemother 1998;10:2661-7.
2. Cox RJ, Sutherland A, Vederas JC. Bacterial diaminopimelate metabolism as a target for antibiotic design. Bioorg Med Chem 2000;8:843-71.
3. Shedlarski JG, Gilvarg C. The pyruvate-aspartic semialdehyde condensing enzyme of Escherichia coli. J Biol Chem 1970;245:1362–73.
4. Tamir H, Gilvarg C. Density gradient centrifugation for the separation of sporulating forms of bacteria. J Biol Chem 1974;249:3034–40.
5. Schrumpf B, Schwarzer A, Kalinowski J, Puhler A, Eggeling L, Sahm H. A functionally split pathway for lysine synthesis in corynebacterium glutamicum. J Bacteriol 1991;173:4510-6.
6. Scapin G, Reddy SG, Zheng R, Blanchard JS. Three-dimensional structure of Escherichia coli dihydrodipicolinate reductase in complex with NADH and the inhibitor 2, 6-pyridinedicarboxylate. Biochemistry 1997;36:15081–8.
7. Cirilli M, Zheng R, Scapin G, Blanchard JS. The three-dimensional structures of the Mycobacterium tuberculosis dihydrodipicolinate reductase-NADH-2, 6-PDC and-NADPH-2, 6-PDC complexes. Structural and mutagenic analysis of relaxed nucleotide specificity. Biochemistry 2003;42:10644–50.
8. Pearce FG, Sprissler C, Gerrard JA. Characterization of dihydrodipicolinate reductase from the rmotogamaritima reveals the evolution of substrate binding kinetics. J Biochem 2008;143:617–23.
9. Coulter CV, Juliet A, Gerrard, James AE, Kraunsoe, Pratt AJ. Escherichia coli dihydrodipicolinate synthase and dihydrodipicolinate reductase: kinetic and inhibition studies of two putative herbicide targets. Pestic Sci 1999;55:887–95.
10. Couper L, McKendrick JE, Robins DJ. Pyridine and piperidine derivatives as inhibitors of dihydrodipicolinic acid synthase, a key enzyme in the diaminopimelate pathway to L-lysine. Bioorg Med Chem Lett 1994;4:2267-72.
11. Giovanna S, Sreelatha GR, Renjian Z, John SB. Three-dimensional structure of escherichia coli dihydrodipicolinate reductase in complex with NADH and the inhibitor 2, 6-Pyridinedicarboxylate. Biochemistry 1997;36:15081-8.
12. Geourjon C, Deleage G. SOPMA: Significant improvements in protein secondary structure prediction by consensus prediction. CABIOS Comput Appl Biosci 1995;11:681-4.
13. Garnier J, Gibrat JF, Robson B. GOR method for predicting protein secondary structure from amino acid sequence. Methods Enzymol 1996;266:540-53.
14. Chou PY, Fasman GD. Prediction of protein conformation. Biochemistry 1974;13:222-45.
15. Thompson JD, Higgins DG, Gibson TJ, Clustal W. Improving the sensitivity of progressive multiple sequence alignment through sequence weighting, position-specific gap penalties and weight matrix choice. Nucleic Acids Res 1994;22:4673-80.
16. Sali A, Blundell TL. Comparative protein modelling by satisfaction of spatial restraints. J Mol Biol 1993;5234:779-815.
17. Kale L, Skeel R, Bhandarkar M, Brunner R, Gursoy A, Krawetz N, *et al*. Schulten KNAMD: Greater scalability for parallel molecular dynamics. J Comput Phys 1999;151:283–12.
18. Schlick T, Skeel R, Brunger A, Kale L, Board JA, Hermans J. Algorithmic challenges in computational molecular biophysics. J Comput Phys 1999;151;9–48.
19. Jorgensen WL, Chandrasekhar J, Madura JD, Impey RW, Klein ML. Comparison of simple potential functions for simulating liquid water. J Chem Phys 1983;79;926–34.
20. Grubmuller H, Heller H, Windemuth A, Schulten K. Generalized verlet algorithm for efficient molecular dynamics simulations with long-range interactions. Mol Simul 1991;6:121–42.
21. Darden TA, Pedersen LG. Molecular modeling: an experimental tool. Environ Health Perspect 1993;101:410-2.
22. Essmann U, Berkowitz ML. Dynamical properties of phospholipid bilayers from computer simulation. Biophys J 1999;76:2081-9.
23. Ryckaert JP, Ciccotti G, Berendsen HJC. Numerical integration of the cartesian equations of motion of a system with constraints: molecular dynamics of n-alkanes. J Comp Physiol 1977;23:327-41.
24. Andersen HC. Rattle: a "velocity" version of the shake algorithm for molecular dynamics calculations. J Comput Phys 1983;52:24-34.
25. Laskoswki RA, MacArthur MW, Moss DS. PROCHECK: A program to check the stereo chemical quality of protein structures. J Appl Crystallogr 1993;26:283-91.
26. Eisenberg D, Luthyand R, Bowie JU. VERIFY3D: assessment of protein models with three-dimensional profiles. Methods Enzymol 1997;277:396-404.
27. Colovos C, Yeates TO. Verification of protein structures: patterns of nonbonded atomic interactions. Protein Sci 1993;2:1511-9.
28. Hooft RW, Vriend G, Sander C. Errors in protein structures. Nature 1996;381:272.
29. Guex N, Peitsh MC. SWISS-MODEL and the swiss-Pdb viewer: an environment for comparative protein modeling. Electrophoresis 1997;15:2714-23.
30. Wolf LK. Chemical engineering news. PyRx Website 2009;87:31.
31. Trott O, Olson AJ. Auto dock vina: improving the speed and accuracy of docking with a new scoring function, efficient optimization, and multithreading. J Comput Chem 2010;31:455–61.
32. DeLano WL. The Py MOL molecular graphics system DeLano scientific, San Carlos, CA, USA; 2012.

How to cite this article

- Bakivijaya Bhaskar, Tirumalasetty Munichandrababu, Netalavasudeva Reddy, Wudayagirirajendra. Homology modeling and development of dihydrodipicolinate reductase inhibitors of *Klebsiellapneumonia*: a computational approach. Int J Curr Pharm Res 2016;8(3):71-76